AN ALGEBRAIC INPUT-OUTPUT EQUATION FOR PLANAR RRRP AND PRRP LINKAGES

Mirja Rotzoll[1], M. John D. Hayes[1], Manfred L. Husty[2]

[1]*Department of Mechanical and Aerospace Engineering, Carleton University, Ottawa, ON K1S 5B6, Canada*
[2]*Unit Geometry and CAD, University of Innsbruck, 6020 Innsbruck, Austria*
Email: Mirja.Rotzoll@carleton.ca; John.Hayes@carleton.ca; Manfred.Husty@uibk.ac.at

ABSTRACT

In this paper the algebraic input-output (*IO*) equations for planar RRRP and PRRP linkages are derived by mapping the linkage displacement constraints into Study's soma coordinates, and using the tangent-half angle substitutions to transform the trigonometric into algebraic expressions. Both equations are found to be equivalent to the one that has already been derived for RRRR linkages, giving exciting new insight into kinematic analysis and synthesis of planar four-bar linkages. The algebraic properties of the *IO* curves of the equations yield information regarding the topology of the linkage, such as the sliding position limits of the prismatic joints and/or the angle limits of the rotational joints. Additionally, the utility of the equations are successfully verified in two approximate synthesis examples.

Keywords: function generator; four-bar linkages; Study soma coordinates.

ÉQUATION ALGÉBRAIQUE D'ENTRÉE-SORTIE POUR DES LIAISONS PLANES RRRP ET PRRP

RÉSUMÉ

Cet article dérive deux équations algébraique d'entrée-sortie pour des liaisons planes RRRP et PRRP en reproduisant le mouvement de liaison dans les coordonnées soma de Study et en utilisant la substitution de demi-angle de tangente pour transformer les expressions trigonométriques en expressions algébriques. Les équations sont déterminées équivalentes à celle qui a déjà été dérivée pour les liaisons RRRR, ce qui permet une utilisation plus large pour la synthèse cinématique. Les courbes des équations fournissent différentes informations sur la topologie de la liaison, telles que la position maximale de glissement de la liaison prismatique ou l'angle maximal de la liaison pivot qui sont discutées dans l'article. En outre, chacune des deux équations ont été vérifiées avec succès grâce à un exemple de synthèse approximant les paramètres de conception optimaux de la liaison.

Mots-clés : liaison mécanique ; mécanisme à quatre barres ; coordonnées soma de Study.

1. INTRODUCTION

In 1954, F. Freudenstein developed an elegant trigonometric equation for planar four-bar linkages connected by four rotational (R) joints [1]. The equation, nowadays known as the *Freudenstein equation*, is widely used in function-generator analysis and synthesis theory, allowing designers to identify the link lengths of mechanisms that optimally transform, typically in a least-squares sense, a specific input angle into a desired output angle governed by a specified functional relation, $f(\psi) = \varphi$. Let d be the distance between the centres of the R-joints connected to the relatively non-moving base; a the driver length, or input link, which is moving with an angle ψ; b the follower length, or output link, which is moving with an angle φ; and c the coupler length of a planar RRRR linkage, as shown in Fig. 1. Then the displacement of the mechanism in terms of the link lengths a, b, c, d, the input angle ψ, and the output angle φ is governed by the following input-output (IO) equation

$$k_1 + k_2\cos(\varphi_i) - k_3\cos(\psi_i) \quad = \quad \cos(\psi_i - \varphi_i). \tag{1}$$

Eq. (1) is linear in the k_i Freudenstein parameters, which are defined in terms of the link length ratios as:

$$k_1 \equiv \frac{(a^2 + b^2 + d^2 - c^2)}{2ab};\ k_2 \equiv \frac{d}{a};\ k_3 \equiv \frac{d}{b}.$$

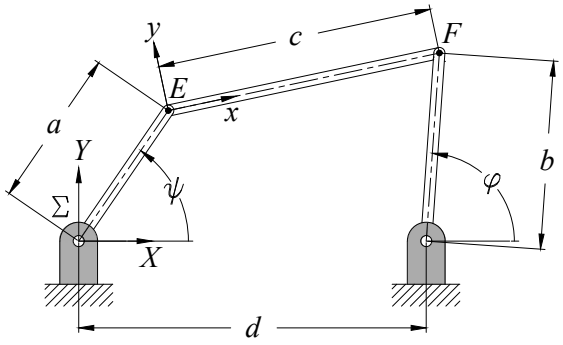

Fig. 1. Planar 4R function generator.

In [2], the authors Hayes, Husty and Pfurner provided an alternative derivation of a general algebraic IO equation for the same type of mechanism:

$$Au^2v^2 + Bu^2 + Cv^2 - 8abuv + D = 0 \tag{2}$$

where

$$\begin{aligned}
A &= (a-b-c+d)(a-b+c+d) = A_1A_2;\\
B &= (a+b-c+d)(a+b+c+d) = B_1B_2;\\
C &= (a+b-c-d)(a+b+c-d) = C_1C_2;\\
D &= (a-b+c-d)(a-b-c-d) = D_1D_2;\\
u &= \tan\frac{\psi}{2};\\
v &= \tan\frac{\varphi}{2}.
\end{aligned}$$

Eq. (2) was obtained by mapping the linkage constraint equations of the input and output links, *i.e.*, circular motion for R-joints, into Study's soma coordinates [3, 4], converting the trigonometric expressions into algebraic ones by applying the tangent of the half-angle substitutions, or Weierstraß substitutions [5], and finally eliminating the Study coordinates to obtain the quartic *IO* curve [2, 6]. The authors of the new *IO* equation believe that their method used to obtain the equation can be further expanded to four-bar mechanisms of any topology for planar, spherical, and spatial cases. Ultimately, this would provide designers with a versatile tool to help them synthesise an optimal mechanism generating an arbitrary function. While others have examined the possibilities of a unified approach to four-bar mechanism synthesis, see [7] for example, proposed methods failed to identify a single algebraic and constraint-based *IO* equation that is truly generalised to four-bars containing two, one, or no prismatic (P) joints.

In this paper we will derive the algebraic *IO* equation for RRRP, and PRRP-linkages using the same technique developed in [2]. The main goal is to demonstrate that the method of deriving the algebraic forms of the *IO* equations using Study's soma and elimination theory [8, 9] lead to precisely the same equation, namely Eq. (2), with only the roles of constant and variable changing for certain design parameters. We will then interpret some important characteristics of the resulting algebraic *IO* curves in the coordinate plane of the input and output variables employing the theory of planar algebraic curves [10–15]. Finally we will illustrate these characteristics in two function generator approximate synthesis examples using the algebraic form of the *IO* equation.

2. ALGEBRAIC *IO* EQUATION FOR RRRP FUNCTION GENERATORS

The planar RRRP-linkage, also called a crank-slider, is a widely used mechanism found in a variety of applications, such as crankshafts, or piston pumps [16]. The linkage transforms a rotational input motion into a reciprocating translational output motion. A schematic of the linkage type is shown in Fig. 2. In the first step, as in the derivation of Eq. (2), the displacement constraints of the driver and follower have to be defined [2, 6]. For that purpose, let Σ_1 be a fixed Cartesian coordinate system at the intersection of the base and driver, E the intersection point of the driver and coupler link, and F the intersection point of the coupler and the follower link. While point E is moving on a circle with a radius of length a around the origin O of Σ_1, F is moving on a line which intersects the baseline at point G making an angle φ at a distance d from

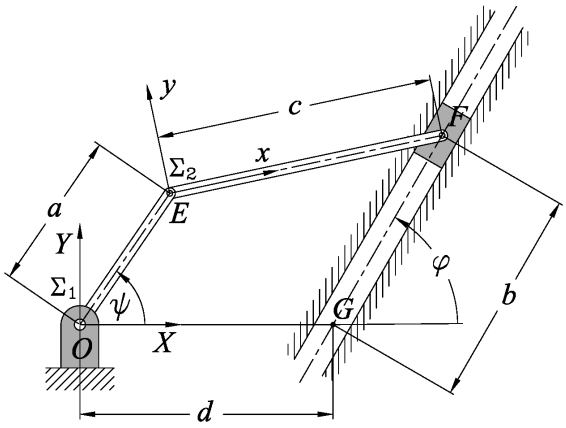

Fig. 2. Planar RRRP function generator.

the origin of Σ_1. Hence, the positions of E and F can be described as points in Σ_1 by the following array

element constraint equations

$$\begin{array}{rcl} X_E - a\cos\psi &=& 0, \\ Y_E - a\sin\psi &=& 0, \end{array} \tag{3}$$

$$\begin{array}{rcl} X_F - d - b\cos\varphi &=& 0, \\ Y_F - b\sin\varphi &=& 0. \end{array} \tag{4}$$

Note that these constraint equations are identical to those formulated for the 4R linkage in [2]. This allows us to proceed in determining the IO equation in the same manner. Let Σ_2 be a moving coordinate frame whose origin is centred at E with x-axis pointing towards F, which moves with the coupler. Then the homogeneous transformation matrix expressed in soma coordinates $(x_0 : x_3 : y_1 : y_2)$ between the two coordinate frames is given by [2]

$$\mathbf{T} \;=\; \frac{1}{x_0^2+x_3^2}\begin{bmatrix} x_0^2+x_3^2 & 0 & 0 \\ 2(-x_0y_1+x_3y_2) & x_0^2-x_3^2 & -2x_0x_3 \\ -2(x_0y_2+x_3y_1) & 2x_0x_3 & x_0^2-x_3^2 \end{bmatrix}. \tag{5}$$

For example, a point (x,y) in Σ_2 can be expressed as a point (X,Y) in Σ_1 by

$$\begin{bmatrix} 1 \\ X \\ Y \end{bmatrix} = \mathbf{T}\begin{bmatrix} 1 \\ x \\ y \end{bmatrix} \tag{6}$$

Now, in the coordinate frame Σ_2 the two end points of the coupler E and F have coordinates $(x,y) = (0,0)$ and $(c,0)$, respectively. These are transformed using Eq. (5) to their representations in Σ_1, and the results are equated to the coordinates for points E and F in Eqs. (3) and (4), which, when simplified, reveal the following four array element position constraint equations in terms of the input and output angles ψ and φ as well as the four soma coordinates:

$$\left.\begin{array}{rcl} -a\cos\psi(x_0^2+x_3^2)+2(-x_0y_1+x_3y_2) &=& 0; \\ -a\sin\psi(x_0^2+x_3^2)-2(x_0y_1+x_3y_2) &=& 0; \\ -(b\cos\varphi+d)(x_0^2+x_3^2)+c(x_0^2-x_3^2)+2(-x_0y_1+x_3y_2) &=& 0; \\ -b\sin\varphi(x_0^2+x_3^2)+2c(x_0x_3)-2(x_0y_2+x_3y_1) &=& 0. \end{array}\right\} \tag{7}$$

The Weierstraß substitutions (tangent of the half angle substitutions)

$$u \;=\; \tan\frac{\psi}{2},\;\; v \;=\; \tan\frac{\varphi}{2}, \tag{8}$$

$$\cos\psi \;=\; \frac{1-u^2}{1+u^2},\;\; \sin\psi \;=\; \frac{2u}{1+u^2}, \tag{9}$$

$$\cos\varphi \;=\; \frac{1-v^2}{1+v^2},\;\; \sin\varphi \;=\; \frac{2v}{1+v^2}, \tag{10}$$

are used to transform the trigonometric constraint based equations in Eq. (7) to algebraic equations. After eliminating the image space coordinates x_i and y_i using resultants and elimination theory, and collecting the results for the variables u and b, the following algebraic IO equation emerges

$$k := \; Au^2b^2 + Bb^2 + Cu^2b - 8abuv + Db + Eu^2 + F \;=\; 0, \tag{11}$$

where

$$\begin{aligned}
A &= v^2+1,\\
B &= v^2+1,\\
C &= -2\,(v-1)\,(v+1)\,(a+d),\\
D &= 2\,(v-1)\,(v+1)\,(a-d),\\
E &= \left(v^2+1\right)(a+c+d)\,(a-c+d),\\
F &= \left(v^2+1\right)(a+c-d)\,(a-c-d).
\end{aligned}$$

By rearranging Eq. (11) it can easily be shown that it is identical to Eq. (2) when the terms multiplying u and v are collected and factored instead of u and b. The difference from a designers' perspective is only that the variables of the 4R linkage are the *IO* angle parameters u and v, while those for the RRRP linkage are the input angle parameter u and output slider distance b.

2.1. Interpretation of the RRRP *IO* Equation

Analysing Eq. (11) using the theory of planar algebraic curves [12] one can see that it has the following characteristics which are independent of the design parameter constants a, c, d, and v.

1. Eq. (11) is of degree $n = 4$ in variables u and b.
2. It contains two double points, $DP = 2$, each located at the intersections with the line at infinity of the u- and b-axis in the $u-b$ variable design parameter plane.
3. It has genus $p = 1$, hence, it is an elliptic curve and the maximum number of assembly modes of the linkage becomes $m = p+1 = 2$ [6, 15].

These three characteristics are now proved to be true for all non-degenerate planar RRRP linkages. The first item is obvious by inspection. The proof of the second item requires that Eq. (11) be homogenised. If we use the the homogenising coordinate w we obtain

$$k_h := Au^2b^2 + Bb^2w^2 + Cu^2bw - 8avubw^2 + Dbw^3 + Eu^2w^2 + Fw^4 = 0. \tag{12}$$

The three partial derivatives of k_h with respect to the three variable coordinates u, b, and w are

$$\left.\begin{aligned}
\frac{\partial k_h}{\partial u} &= 2Aub^2 + 2Cubw - 8avbw^2 + 2Euw^2 &&= 0,\\
\frac{\partial k_h}{\partial b} &= 2Au^2b + 2Bbw^2 + Cu^2w - 8avuw^2 + Dw^3 &&= 0,\\
\frac{\partial k_h}{\partial w} &= 2Bb^2w + Cu^2b - 16avubw + 3Dbw^2 + 2Eu^2w + 4Fw^3 &&= 0.
\end{aligned}\right\} \tag{13}$$

Equations (12) and (13) have two common solutions which are independent of the link lengths a, c, and d, as well as angle parameter v, which are embedded in the coefficients A, B, C, D, E, and F:

$$S_1 := \{u = 1, b = 0, w = 0\}, \quad S_2 := \{u = 0, b = 1, w = 0\}. \tag{14}$$

These two points, called *double points*, common to all algebraic *IO* curves for every planar RRRP four-bar mechanism are the points on the line at infinity $w = 0$ of the u- and b-axes, respectively. Each of these

double points can have real or complex tangents depending on the values of the link lengths, which in turn determines the nature of the mobility of the linkage. Since these two points are uniquely defined relative to the regular points on the curve, they are also known as *singular points*.

The discriminant of Eq. (12) evaluated at a double point reveals whether that double point has a pair of real or complex conjugate tangents [14], yielding information about the topology of the mechanism [6, 13]. If the tangents are complex conjugates the double point is an acnode: a *hermit* point that satisfies the equation of the curve but is isolated from all other points on the curve. If this is the case then the slider travel, represented by b, is restricted. The discriminant and the meaning of its value are [13, 14]

$$\Delta = \left(\frac{\partial^2 k_h}{\partial u \partial w}\right)^2 - \frac{\partial^2 k_h}{\partial u^2}\frac{\partial^2 k_h}{\partial w^2} \quad \begin{cases} > 0 \Rightarrow \text{two real distinct tangents (crunode)}, \\ = 0 \Rightarrow \text{two real coincident tangents (cusp)}, \\ < 0 \Rightarrow \text{two complex conjugate tangents (acnode)}. \end{cases} \tag{15}$$

For the homogeneous IO equation of an RRRP linkage, Eq. (12), the discriminant of the point at infinity $(u:b:w) = (0:1:0)$ on the b-axis is

$$\Delta = -4(v^2+1)^2, \tag{16}$$

meaning that the double point associated with the output slider is always an acnode independently of the link lengths and orientation of the slider. It should not surprise that the Δ of Eq. (12) is always negative, since the slider must always have finite translation limits.

To determine whether the rotational input link is a crank or a rocker, it is sufficient to determine if the numerical value of the coefficient E in Eq. (11) is less than zero when the coordinates in Σ_1 are transformed by the rotation about O_{Σ_1} required to make $v = 1$, *i.e.*, $\varphi = \pi/2$. Since the two factors (v^2+1) and $(a+c+d)$ in E must always be greater than zero, it is a simple matter to show that the condition for input link a to be a crank reduces to

$$a - c + d \quad < \quad 0. \tag{17}$$

The proof for the third item comes from the definition of genus, which in this case is the difference between the maximum number of double points for a curve of degree 4 and the actual number of double points it possesses. The maximum number of double points, DP_{max} for an algebraic curve of degree n is given by [17]

$$DP_{max} \quad = \quad \frac{1}{2}(n-1)(n-2).$$

The maximum number of double points for a curve of degree 4 is 3. We see that because the algebraic IO curve has only 2 double points, it is deficient by 1, hence it's genus is $p = 1$. Because of this, it cannot be parameterised, and it is defined to be an *elliptic* curve [12]. This definition does not mean that the curve has the form of an ellipse, rather that the curve can be expressed, with a suitable change of variables, as an elliptic curve. In the plane, every elliptic curve with real coefficients can be put in the standard form

$$x_2^2 \quad = \quad x_1^3 + Ax_1 + B$$

for some real constants A and B. We now consider some illustrative RRRP examples.

Example 1. Design parameter selection: $a = 2.8$; $c = 1.7$; $d = 1$; $v = 1.5$.

With the chosen design parameters, the input link a is a rocker because Eq. (17) is > 0 for some $-\pi \leq \psi \leq \pi$. Two different assembly modes I and II can be identified examining Fig. 3. Each assembly mode has two locations where the mechanism is positioned at an input singular configuration where the tangents

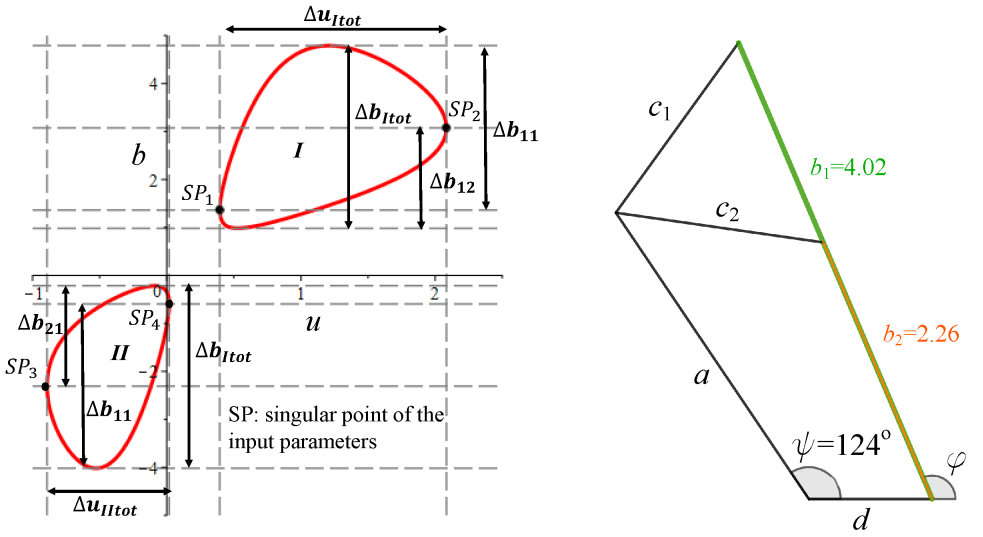

Fig. 3. RRRP where $a = 2.8$, $c = 1.7$, $d = 1$, $v = 1.5$.

of the IO equation are vertical, separating each assembly mode into two working modes. If the link is assembled according to the upper right part of the curve (assembly mode I), Δu_{Itot} and Δb_{Itot} correspond to the maximum swing angle and maximum sliding position, respectively. Considering each working mode separately, Δb_{11} and Δb_{12} correspond to the maximum sliding position in assembly mode I. Similarly, if the link is assembled according to the lower left part of the curve (assembly mode II), Δu_{IItot} and Δb_{IItot} correspond to the maximum swing angle and maximum sliding position. The maximum sliding positions for each working mode are Δb_{21} and Δb_{22}.

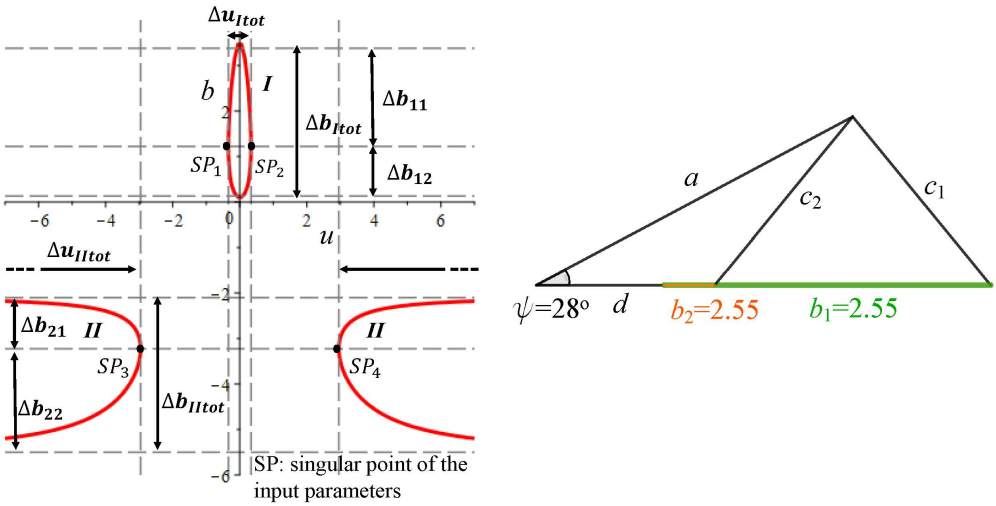

Fig. 4. RRRP where $a = 2.8$, $c = 1.7$, $d = 1$, $v = 0$.

Example 2. Design parameter selection: $a = 2.8$; $c = 1.7$; $d = 1$; $v = 0$.

Taking the same design parameters, but changing the orientation of the slider to $v = 0$ reveals a representation of the IO equation as shown in Fig. 4. Again, examining Eq. (17) shows that the expression is not < 0 for every $-\pi \leq \psi \leq \pi$, hence, the input link is a rocker. The linkage is once again split into two assembly modes, I and II. Due to the chosen parametrisation according to Eq. (8) and as $\psi = \pi$ is included in assembly mode I, the graph contains the point at $u = \pm\infty$, explaining the asymptotes of the IO equation. The maximum swing angle as well as the maximum sliding position can be evaluated analogous to the previous example.

Example 3. Design parameter selection: $a = 2$; $c = 2.5$; $d = 1$; $v = 0.2$.

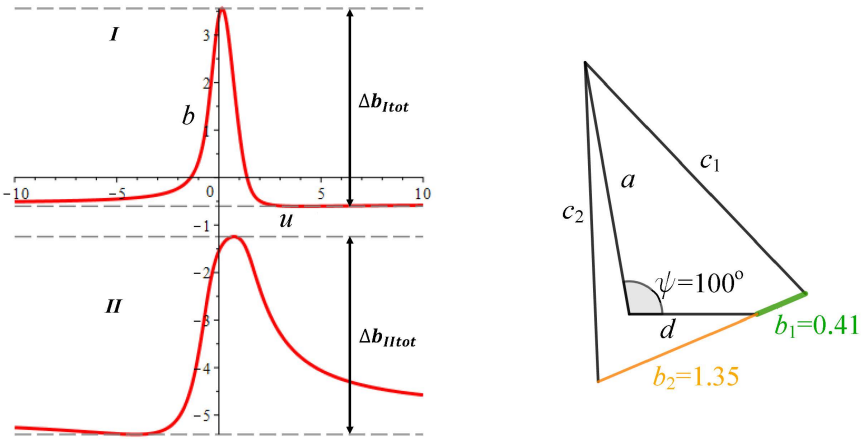

Fig. 5. RRRP where $a = 2$, $c = 2.5$, $d = 1$, $v = 0.2$.

These design parameters yield an IO equation illustrated in Fig. 5. In contrast to the previous examples, Eq. (17) is < 0 meaning that the input link a can fully rotate. This linkage also possesses two assembly modes I and II, resulting in identical maximum sliding position, $\Delta b_{Itot} = \Delta b_{IItot}$. In this example, points where the mechanism is located at an input singular configuration do not exist. The output linkage movement is unambiguously defined via the linkage assembly.

Example 4. A very special RRRP linkage arises when $a = c$ and $v = 0$. With these conditions, the factors of Eq. (11) simplify to

$$(b+d)(bu^2+2cu^2+du^2+b-2c+d) = 0. \tag{18}$$

As a result, this special IO equation is decomposed into two operation modes. Moreover, two additional double points can be observed. These double points, the bifurcation points, BP_1 and BP_2, are always located at

$$BP_1(+1,-d), \qquad BP_2(-1,-d).$$

This IO equation has four different working modes, the input link a is able to rotate completely, and the mechanism has the ability to fold. From Eq. (18), the global maximum is found at $b_{max} = 2c - d$ and the global minimum is the asymptote at $b_{max} = -2c - d$ which leads to the following four maximum sliding positions $\Delta b_{i_{max}}$

$$\Delta b_{1_{max}}, = 4a = 4c \qquad \Delta b_{2_{max}}, = 2c \qquad \Delta b_{3_{max}}, = 2c \qquad \Delta b_{4_{max}}, = 0. \tag{19}$$

An example of the IO equation (where $a = c = 1.7$ and $d = 1$) is illustrated in Fig. 6.

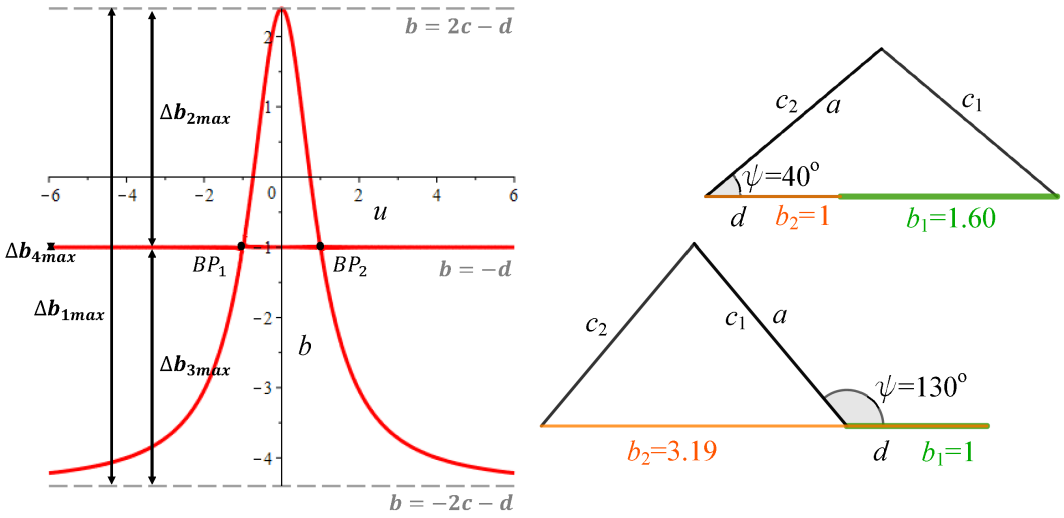

Fig. 6. RRRP where $a = c = 1.7$, $d = 1$, $v = 0$.

2.2. RRRP Approximate Synthesis

To show that Eq. (11) can be used to generate arbitrary functions of the form $f(\psi) = b$, an example approximating the curve

$$b = cos(\psi) \tag{20}$$

is considered. For this example, 50 sample points were evenly distributed within the interval $-3 \leq u \leq 3$.

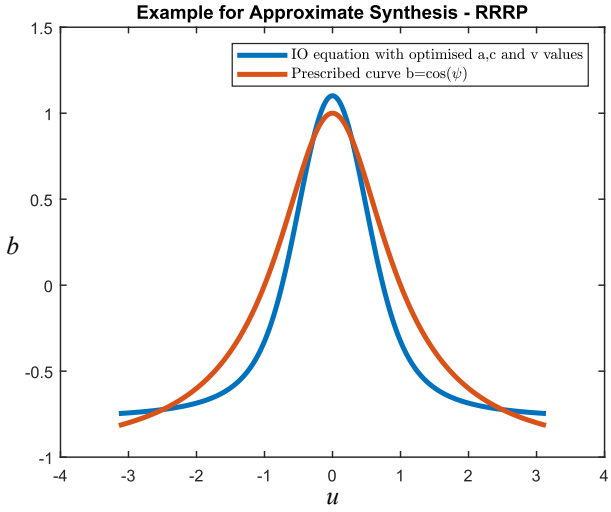

Fig. 7. $a = 0.9426$, $c = 1.1587$, $d = 1$, $v = 1.5 \times 10^{-5}$.

The Newton-Gauss algorithm was used to iteratively minimise the structural error, the error residual found between the prescribed curve and the curve generated by the linkage [18]. The optimised function approximation with an RRRP linkage is obtained with the identified design parameters $a = 0.9426$, $c = \pm 1.1587$, $d = 1$, and $v = \pm 1.5 \times 10^{-5}$. Fig.7 illustrates the structural error of the identified linkage. This

example underscores the applicability of the general algebraic *IO* equation for RRRP in addition to RRRR linkages.

3. ALGEBRAIC EQUATION FOR PRRP FUNCTION GENERATOR

As it was demonstrated that the general algebraic *IO* equation is useful for RRRP mechanism synthesis, it is reasonable to expect that the equation is equally valid for PRRP mechanisms. We won't consider mechanisms with three P-joints since such linkages can only generate translations. The PRRP mechanism consists of one prismatic, two rotational, and another prismatic joint. In addition to a translational output motion b, the input motion a of the function generator is also a translation governed by a functional relation expressed by $f(a) = b$. The most common configuration is the elliptical trammel whose prismatic joint directions are perpendicular to each other, but the P-joint axes may have any non zero angle between them, as illustrated in Fig. 8.

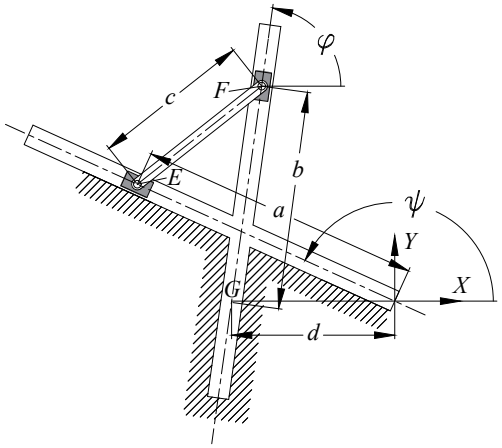

Fig. 8. A PRRP linkage.

Since the two prismatic joints are both moving on a line, the initial constraint equations for the PRRP can again be set up according to Eqs. (3) and Eqs. (4). Note that in this particular case, the variables of the *IO* equation become a and b, while u, v, c, and d represent the design parameters. According to the same derivation for the RRRP and the RRRR function generators, but instead treating both a and b as variables, the *IO* equation of the function generator becomes

$$Aa^2 + Bb^2 + Cab + Da + Eb + F = 0, \tag{21}$$

where the coefficients are factors of constants u, c, d, and v:

$$\begin{aligned}
A &= \left(v^2+1\right)\left(u^2+1\right);\\
B &= \left(v^2+1\right)\left(u^2+1\right);\\
C &= -2\left(uv-u+v+1\right)\left(uv+u-v+1\right);\\
D &= 2d\left(v^2+1\right)\left(u-1\right)\left(u+1\right);\\
E &= -2d\left(v-1\right)\left(v+1\right)\left(u^2+1\right);\\
F &= -\left(v^2+1\right)\left(u^2+1\right)\left(c-d\right)\left(c+d\right).
\end{aligned}$$

Again, by collecting the variables in a different way it can easily be shown that Eq. (21) is identical to Eqs. (2) and (11).

3.1. Interpretation of the PRRP *IO* Equation

Eq. (21) has the following characteristics.

1. It is of degree $n = 2$.
2. It is a quadratic equation in two variables, thus, the *IO* equation is a conic section.
3. It's *IO* curve possesses genus $p = 0$, hence the maximum number of assembly modes of the linkage is $m = p + 1 = 1$ [6, 15].

From the discriminant, Δ_q, of the quadratic form associated with the conic section implied by Eq. (21)

$$\Delta_q = \begin{vmatrix} A & C/2 \\ C/2 & B \end{vmatrix}, \tag{22}$$

we can, according to Tab. 1, determine whether the conic is an ellipse, parabola or hyperbola [19]. For

Discriminant of a non-degenerated conic	Shape
$\Delta_q > 0$	ellipse
$\Delta_q = 0$	parabola
$\Delta_q < 0$	hyperbola

Table 1. Impact of the discriminant value on the shape of function the PRRP can generate.

Eq. (21) the discriminant reduces to

$$\begin{vmatrix} \left(v^2+1\right)\left(u^2+1\right) & -\left(uv-u+v+1\right)\left(uv+u-v+1\right) \\ -\left(uv-u+v+1\right)\left(uv+u-v+1\right) & \left(v^2+1\right)\left(u^2+1\right) \end{vmatrix} = 4\left(uv+1\right)^2\left(u-v\right)^2 \tag{23}$$

Since Eq. (23) is independent of link lengths then $\Delta_q \geq 0$ for all PRRP linkages and the conic represented by Eq. (21) can never be an hyperbola. The graph of the *IO* equation is always an ellipse with but one exception: if $u = -\frac{1}{v}$ or $u = v$, the conic becomes a special parabola, *i.e.*, two parallel lines. A distinguished ellipse, the circle, arises when $A = B$ and $C = 0$ which are the cases for

$$u = \pm 1, v = 0 \qquad\qquad u = 0, v = \pm 1, \tag{24}$$

i.e., when the axes are perpendicular to each other. These findings align with the literature [20] proving that this type of mechanism generates an ellipse, confirming the validity of the derived PRRP *IO* equation.

Example 5. Design parameter selection: $v = 1.7$; $u = 0.8$; $c = 2$; $d = 1$.

Fig. (9) illustrates the maximum sliding positions a_{tot} and b_{tot}. Considering a to be the input slider, two singular points separate the curve into two working modes. Hence, the output slider can have two different maximum sliding positions Δb_1 and Δb_2.

3.2. PRRP Approximation Synthesis

To show that Eq. (21) can also be used to generate a general function $f(a) = b$, we now consider an example where the desired function is

$$b = cos(a). \tag{25}$$

For this example 50 sample points are selected to be evenly distributed within the interval $0 \leq a \leq 2$. Again, the Newton-Gauss algorithm is used to minimise the structural error.As a result, the best approximation with a PRRP linkage is obtained with the identified constants $c = 2.0313$, $d = 1$, $u = -1.1868$, and $v = 0.1353$,

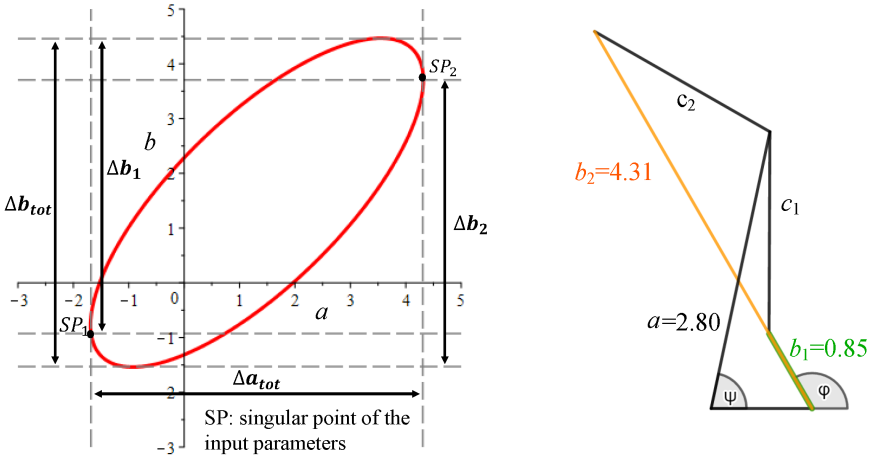

Fig. 9. PRRP where $v = 1.7$, $u = 0.8$, $c = 2$, $d = 1$.

or $c = 2.0313$, $u = 1.1868$ and $v = -0.1353$. The designer may chose between these two different assembly modes. The structural error is illustrated in Fig. 10. The desired curve is illustrated in red, and the blue curve represents the approximation obtained by the PRRP linkage. For this example, the approximation obtained by the PRRP function generator is notably close to the prescribed curve. Hence, this example confirms the applicability of Eq. (21) for approximate synthesis problems.

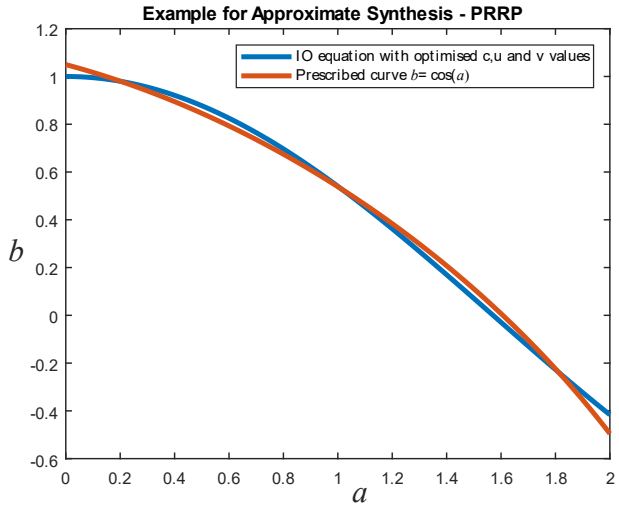

Fig. 10. PRRP: $v = 0.1353$, $u = -1.1868$, $c = .03132$, $d = 1$.

4. CONCLUSIONS

In this paper two algebraic *IO* equations for RRRP and PRRP linkages were derived. It was shown that these equations are identical to the algebraic equation for RRRR linkages derived in [2]. We believe this to be a remarkable result having never been reported in the vast body of archival literature collected since antiquity! Analysing the equations revealed that the RRRP linkage can have a maximum of two assembly

modes which can be divided into two working modes. A folding mechanism occurs if $a = c$ and $v = 0$. The PRRP linkage has only one assembly mode. It was demonstrated that its *IO* curve is either an ellipse or if $u = -\frac{1}{v}$ or $u = v$ two parallel lines. Furthermore, both equations were verified by a synthesis example that approximated the respective design parameters. Being able to expand the algebraic *IO* equation to two additional linkages, RRRP and PRRP, helps designers to choose the optimal linkage with the optimal design parameters with reduced time and effort. The generalisation of this paper is an important step towards the main goal of synthesising the optimal linkage of planar, spherical, or spatial function generators.

ACKNOWLEDGEMENTS

The authors gratefully acknowledge the partial financial support of this research by Mitacs Canada through a Globalink Research Grant awarded to the first author.

REFERENCES

1. Freudenstein, F. *Design of Four-link Mechanisms.* Ph.D. thesis, Columbia University, New York, N.Y., USA, 1954.
2. Hayes, M.J.D., Husty, M.L. and Pfurner, M. "Input-output Equation for Planar Four-bar Linkages." In "International Symposium on Advances in Robot Kinematics," pp. 12–19. Springer, 2018.
3. Study, E. *Geometrie der Dynamen*. Teubner Verlag, Leipzig, Germany, 1903.
4. Bottema, O. and Roth, B. *Theoretical Kinematics*. Dover Publications, Inc., New York, NY, U.S.A., 1990.
5. Bradley, G.L. and Smith, K.J. *Calculus*. Prentice Hall, Englewood Cliffs, NJ, U.S.A., 1995.
6. Husty, M.L. and Pfurner, M. "An Algebraic Version of the Input-output Equation of Planar Four-bar Mechanisms." pp. 746–757. *International Conference on Geometry and Graphics*, Milan, Italy, 2018.
7. Bai, S. and Angeles, J. "A Unified Input-output Analysis of Four-bar Linkages." *Mechanism and Machine Theory*, Vol. 43, No. 2, pp. 240–251, 2008.
8. Salmon, G. *Lessons Introductory to the Modern Higher Algebra,* 4^{th} edition. Hodges, Foster, and Figgis, Dublin, Rep. of Ireland, 1885.
9. Cox, D., Little, J. and O'Shea, D. *Ideals, Varieties, and Algorithms: an Introduction to Computational Algebraic Geometry and Commutative Algebra,* second edition. Springer-Verlag, Berlin, Germany, 1997.
10. Salmon, G. *A Treatise on Conic Sections,* 6^{th} edition. Longmans, Green, and Co., London, England, 1879.
11. Salmon, G. *A Treatise on the Higher Plane Curves,* 3^{rd} edition. Hodges, Foster, and Figgis, Dublin, Rep. of Ireland, 1879.
12. Primrose, E. *Plane Algebraic Curves*. MacMillan, 1955.
13. Hilton, H. *Plane Algebraic Curves*. Clarendon Press, Oxford, England, 1920.
14. Husty, M., Karger, A., Sachs, H. and Steinhilper, W. *Kinematik und Robotik*. Springer-Verlag Berlin Heidelberg New York, 1997.
15. Harnack, A. "Über die Vielteiligkeit der ebenen algebraischen Kurven." In "Mathematische Annalen," pp. 189–198, 1876.
16. Wunderlich, W. *Ebene Kinematik*. Hochschultaschenbücher-Verlag, Mannheim, Wien, Zürich, 1970.
17. Hunt, K. *Kinematic Geometry of Mechanisms*. Clarendon Press, Oxford, England, 1978.
18. Tinubu, S. and Gupta, K. "Optimal Synthesis of Function Generators Without the Branch Defect." *Journal of Mechanisms, Transmissions, and Automation in Design*, Vol. 106, No. 3, pp. 348–354, 1984.
19. Glaeser, G., Stachel, H. and Odehnal, B. *The Universe of Conics: From the Ancient Greeks to* 21^{st} *Century Developments*. Springer, 2016.
20. Sangwin, C. "The Wonky Trammel of Archimedes." *Teaching Mathematics and Its Applications: International Journal of the IMA*, Vol. 28, No. 1, pp. 48–52, 2009.